

**Application of the NIOSH-Modified Holmberg-Persson Approach to Perimeter Blast Design**  
by  
Stephen Iverson, Chuck Kerkering, William Hustrulid  
NIOSH/SRL

**Abstract**

Perimeter control blasting is common in civil construction projects but not as common in mining. A poorly designed and executed underground mine development blast design can result in unwanted wall rock damage. This damage increases the risk of rock falls and injury. With the availability of good drilling equipment, it is a simple matter to add the few extra holes needed to change conventional drifting into drifting with perimeter control.

In the 1970's, Holmberg and Persson (H-P) introduced the Swedish approach to contour blasting and it has found wide acceptance due to the logical basis and ease of application. An error in the mathematics of the H-P approach was discovered in 2002 and use has fallen into question.

This paper presents a modification which corrects the mathematical error. The NIOSH-modified H-P design curves are basically identical to the original ones in the far field but with some significant differences in the near field. The application of the curves remains the same. The determination of the required site constants and the construction of the design curves are demonstrated with respect to data collected at the Stillwater mine, Nye, Montana.

*The findings and conclusions in this report are those of the authors and do not necessarily represent the views of the National Institute for Occupational Safety and Health.*

## **1. Introduction**

In underground mine development, poorly designed and executed blast designs can result in unwanted wall rock damage which increases the risk for injury while, at the same time, adds mining costs. Perimeter control blasting techniques are regularly employed in civil construction projects where the economic penalties for over-break and even under-break can be severe. Although perhaps not so direct or obvious as in civil construction, adverse consequences are also associated with poor excavation practices in mining. In the past, an obstacle to the use of perimeter control blasting has been the reluctance on the part of mine owners/operators to invest in modern drilling equipment. It is difficult to introduce precision blasting when the drilling is done based upon the use of jack-legs. Fortunately, most operators today recognize the overall economies inherent in the use of drill jumbos. With the availability of good drilling equipment, it is a simple matter to add the few extra holes needed to change conventional drifting into drifting with perimeter control. Being able to count on properly positioned and oriented holes is an enormous advantage to the blast designer. With the wide assortment of explosive products available today, the blast designer has nearly too many options. Soundly-based but easy to use blast design tools are needed if perimeter control blasting is to be widely adopted in practice.

In the late 1970's, Holmberg and Persson (H-P) introduced the Swedish approach to contour blasting (Holmberg and Persson (1978, 1979), Holmberg (1982)). Since that time, its use has found quite wide acceptance due to the logical basis and the relative ease of application. However, an error in the mathematics behind the H-P design curves was discovered in 2002 (Hustrulid and Lu, 2002) and the use of the approach has fallen into question.

This paper begins with a review of the H-P approach and provides a modification which corrects the mathematical error. The construction of the NIOSH-modified H-P design curves are then demonstrated for the same charge geometry and charge concentrations used by H-P. It will be seen that the curves are nearly identical to the original H-P curves in the far field but with some significant differences in the near field. The application of the curves remains the same.

The H-P approach is based upon rock damage being related to peak particle velocity. The basic equation upon which the design curves are based is:

$$\text{PPV} = K Q^\alpha / R^\beta \quad (1)$$

Where:

K,  $\alpha$ ,  $\beta$  = constants  
PPV = peak particle velocity  
Q = charge weight  
R = distance

Hence, a necessary part of the approach is to determine the required constants K,  $\alpha$ , and  $\beta$  for the particular site. In the second part of the paper, a set of procedures for extracting these constants from the seismic signals obtained during drifting at the Stillwater mine, Nye, Montana will be demonstrated. The blast design curves using the NIOSH-modified H-P approach will be developed using the derived constants.

To be able to apply the curves for perimeter control blast design, knowledge of the limiting PPV is required. In the case of Stillwater, the PPV limit with respect to over-break has been determined using the design curves together with laser scanner measurements.

The paper concludes with some comments regarding future work.

## **2. The NIOSH-Modified Holmberg-Persson Perimeter Blast Design Approach**

Damage to structures due to surface blasting has been found to be related to the peak particle velocity (PPV) associated with the blast-produced seismic wave. As indicated in the Introduction, the general equation is

$$PPV = KQ^\alpha / R^\beta \quad (1)$$

Where:

PPV = peak particle velocity

Q = charge weight/delay

R = distance

K,  $\alpha$ ,  $\beta$  = constants

By analyzing the results of a large set of surface blasting measurements performed by the U.S. Bureau of Mines, Lundborg et al (1978) found that they could be well described using

$$K = 700$$

$$\alpha = 0.7$$

$$\beta = 1.5$$

In this case, the charge weight Q is expressed in kilograms, the distance R is expressed in meters, and the resulting PPV is expressed in mm/s. Holmberg and Persson (Holmberg and Persson, 1978) applied equation (1) to examining the damage produced to the surrounding rock mass when using long cylindrical charges. They divided the long charge into a number (n) of small elemental charges of equal length  $\Delta L$ . Assuming that the charge concentration per unit length is q, one can express the charge weight  $\Delta Q$  for each element as

$$\Delta Q = q \Delta L \quad (2)$$

Where

$\Delta Q$  = charge weight of each elemental charge

$\Delta L$  = length of each elemental charge

q = charge concentration per unit length

The peak particle velocity at a given observation point due to the arrival of a particular elemental charge (denoted by the subscript i) may be expressed by

$$\Delta PPV_i = K (\Delta Q)^{\alpha} / R_i^{\beta} = K (q \Delta L)^{\alpha} / R_i^{\beta} \quad (3)$$

To simplify the discussion, the particular geometrical situation shown in Figure 1 will be assumed.

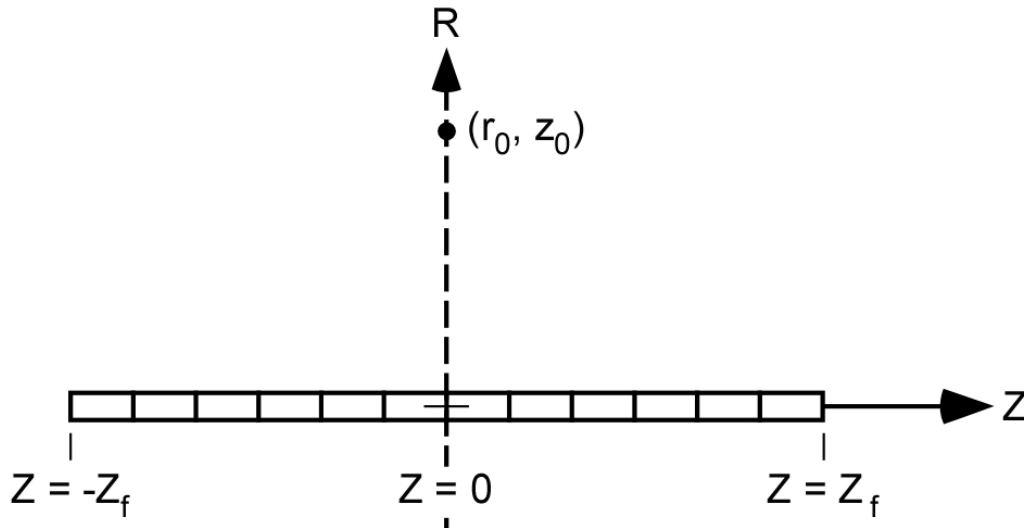


Figure 1. Diagrammatic representation of the simplified charge – observer geometry used in the examples.

As can be seen, the charge lies along the z axis with the r axis passing through the mid-point of the charge. The total PPV due to the arrival of the seismic waves from the different elemental charges is to be determined at an observation point ( $z_0, r_0$ ) located along the r axis. Since the waves from the elemental charges travel different distances to reach the observation point, their amplitudes will be distance dependent. Also, in general, the arrival times and wave orientation will vary depending on the explosive velocity of detonation and the wave velocity through the rock mass. In their approach, Holmberg and Persson have assumed:

1. The entire charge detonates instantaneously
2. The amplitudes are simply summed without considering arrival direction

This simplifies the situation considerably. The resulting PPV is obtained by summing the contributions from the different elemental charges.

$$PPV = \sum_1^n \Delta PPV_i = K q^\alpha \sum_1^n (\Delta L)^\alpha / (R_i)^\beta \quad (4)$$

Holmberg and Persson replaced the summation by the following integral expression

$$PPV = K \left\{ q \int_{z_i}^{z_f} \frac{dz}{[(r - r_o)^2 + (z - z_o)^2]^{(\beta/2)\alpha}} \right\}^\alpha \quad (5)$$

For the case shown in Figure 1,

$$r = 0$$

$$z_o = 0$$

Thus equation (5) becomes

$$PPV = K \left\{ q \int_{z_i}^{z_f} \frac{dz}{[(r_o)^2 + (z)^2]^{\beta/2\alpha}} \right\}^\alpha \quad (6)$$

The integral can be numerically evaluated. The results for a 3m long charge ( $z_i = -1.5$  m and  $z_f = 1.5$  m) assuming that

$$K = 700$$

$$\alpha = 0.7$$

$$\beta = 1.5$$

are shown in Figure 2 for five values of  $q$ :

$$\begin{aligned} q &= 2.5 \text{ kg/m} \\ q &= 1.5 \text{ kg/m} \\ q &= 1.0 \text{ kg/m} \\ q &= 0.5 \text{ kg/m} \\ q &= 0.2 \text{ kg/m} \end{aligned}$$

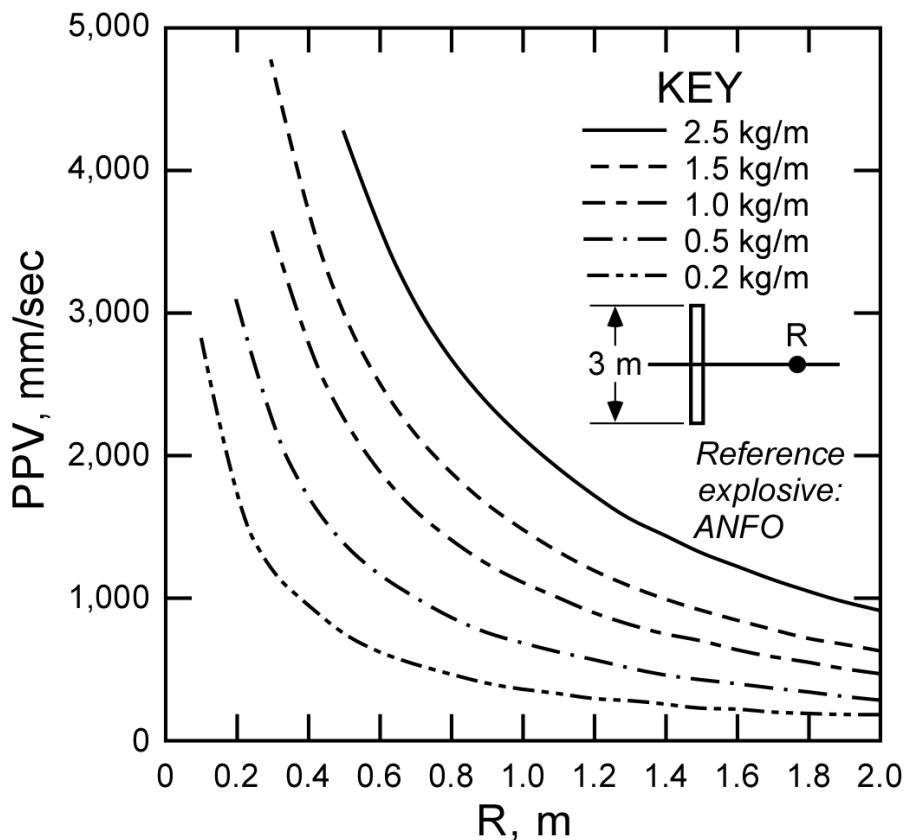


Figure 2. Peak particle velocity versus distance as a function of charge concentration. Charge length = 3 m, observation axis along charge mid-plane. After Holmberg (1982).

In the figure, the symbol R has been used in place of  $r_o$  in keeping with H-P convention. To be able to use these curves for design, one must determine the PPV value associated with unacceptable damage. Over-break would be one type of such damage. Assume that the measured over-break for a fully charged wall hole ( $q = 1.0 \text{ kg/m}$ ) is 0.5 m. This experience point is shown in Figure 3. In this case, the corresponding PPV over-break limit would be of 2230 mm/sec. If it was desired to keep the over-break to 0.15 m or less, based upon the curves, the charge concentration in the perimeter holes should be reduced to 0.2 kg/m or less. This is a very easy to use perimeter blast design procedure and has found wide acceptance since its introduction in 1978.

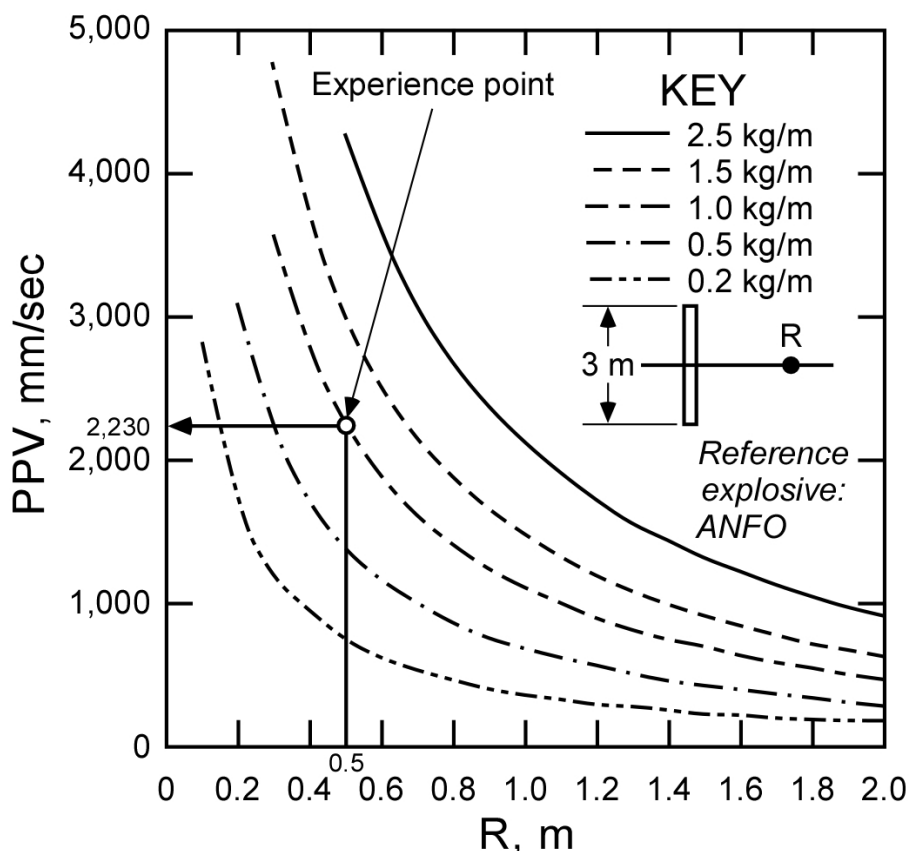


Figure 3. Addition of the experience point to the peak particle velocity versus distance curves of Figure 2.

Unfortunately, as Hustrulid and Lu (2002) have pointed out, the step going from PPV expressed as a summation in equation (4) to PPV expressed by the integral in equation (5) is not correct. The exponent  $\alpha$  has been moved from inside the summation sign to outside of the integral sign. Hence the curves shown in Figure 3 are not correct. Okay, one might say, we will simply revert back to using the summation expression, equation (4).

$$PPV = \sum_1^n \Delta PPV_i = Kq^\alpha \sum_1^n (\Delta L)^\alpha / (R_i)^\beta \quad (4)$$

Since  $\Delta L$  is the same for all of the elemental charges, this term can be removed from under the summation sign to yield

$$PPV = \sum_1^n \Delta PPV_i = Kq^\alpha (\Delta L)^\alpha \sum_1^n 1 / (R_i)^\beta \quad (7)$$

It appears that one simply needs to determine the radial distance  $R_i$  from the observation point to the mid-point of each elemental charge, form the inverse, raise it to the power  $\beta$  and then to sum all of the contributions. However, by closely examining equation (7), it is clearly seen that the PPV depends upon the length of the elemental charge raised to the power  $\alpha$ . Only for the very special case,  $\alpha = 1$ , the

equation is stable. For the case  $\alpha > 1$ , the PPV decreases to zero as the elemental length decreases. For the case  $\alpha < 1$ , the PPV increases to infinity as the elemental length decreases. Thus, this procedure cannot be followed.

To try and retain the ease and simplicity of the Holmberg-Persson approach while correcting the mathematical problems, NIOSH has revisited the basic concepts involved.

Retaining the basic H-P assumptions:

1. The entire charge detonates instantaneously
2. The amplitudes are simply summed without considering arrival direction

the new solution involves determining the average travel distance  $\bar{R}$  to the observation position for all of the elemental charges. Once  $\bar{R}$  has been determined, the PPV is obtained using

$$\text{PPV} = K Q^\alpha / \bar{R}^\beta = K (qL)^\alpha / \bar{R}^\beta \quad (8)$$

The average travel distance,  $\bar{R}$ , is, by definition (Martin, 2007),

$$\bar{R} = \frac{1}{L} \int_{z_i}^{z_f} [(z - z_o)^2 + (r - r_o)^2]^{1/2} dz \quad (9)$$

Where:

$$L = z_f - z_i$$

The value of the indefinite integral may be written as (Weast, 1983)

$$\int \sqrt{(z - z_o)^2 + (r - r_o)^2} dz = \frac{1}{2} \left[ (z - z_o) \sqrt{(z - z_o)^2 + (r - r_o)^2} + (r - r_o)^2 \log_e((z - z_o) + \sqrt{(z - z_o)^2 + (r - r_o)^2}) \right]$$

For the case of a charge located along the z-axis, centered at the origin, and with the observation position designated as  $(r_o, z_o)$ , one finds that

$$r = 0$$

and

$$z_o = 0$$

Hence, the indefinite integral may be written as

$$\int \sqrt{z^2 + r_o^2} dz = \frac{1}{2} \left[ z \sqrt{z^2 + r_o^2} + r_o^2 \log_e(z + \sqrt{z^2 + r_o^2}) \right] \quad (10)$$

For the example case of the 3m long charge,

$$\begin{aligned} z_i &= -1.5 \text{ m} \\ z_f &= 1.5 \text{ m} \end{aligned}$$

the definite integral becomes

$$\int_{z_i}^{z_f} \sqrt{z^2 + r_o^2} dz = \frac{1}{2} \left[ z_f \sqrt{z_f^2 + r_o^2} + r_o^2 \log_e(z_f + \sqrt{z_f^2 + r_o^2}) \right] - \frac{1}{2} \left[ z_i \sqrt{z_i^2 + r_o^2} + r_o^2 \log_e(z_i + \sqrt{z_i^2 + r_o^2}) \right]$$

Substituting the values for  $z_i$  and  $z_f$ , one finds

$$\int_{-1.5}^{1.5} \sqrt{z^2 + r_o^2} dz = \frac{1}{2} \left[ 1.5 \sqrt{1.5^2 + r_o^2} + r_o^2 \log_e(1.5 + \sqrt{1.5^2 + r_o^2}) \right] - \frac{1}{2} \left[ -1.5 \sqrt{(-1.5)^2 + r_o^2} + r_o^2 \log_e(-1.5 + \sqrt{(-1.5)^2 + r_o^2}) \right]$$

The value of the integral is then evaluated for chosen values of  $r_o$ . For example, when

$$r_o = 2 \text{ m}$$

the value of the integral (Int) becomes

$$\text{Int} = 6.5225$$

The corresponding value of  $\bar{R}$  is

$$\bar{R} = \text{Int}/L = 6.5225/3 = 2.174 \text{ m}$$

Assuming that

$$\begin{aligned} q &= 1 \text{ kg/m} \\ K &= 700 \\ \alpha &= 0.7 \\ \beta &= 1.5 \end{aligned}$$

the calculated value of PPV is

$$\text{PPV} = K (qL)^\alpha / \bar{R}^\beta = 700 (1 \times 3)^{0.7} / 2.174^{1.5} = 471 \text{ mm/s}$$

The process can then be repeated for different values of  $q$  and  $r_o$  to obtain a set of design curves. These are shown in Figure 4 for the same  $q$  values as chosen by Holmberg-Persson. When  $r_o = 0$ , the observer would be at the charge midpoint and  $\bar{R} = L/4$ . In comparing the NIOSH-modified with the original Holmberg-Persson results, it is observed that the agreement is quite good in the far-field (for  $r_o > 1\text{m}$ ,  $r_o > L/3$ ). However, as one approaches the charge axis, the differences increase. The experience point, assuming as before that the observed over-break for a fully charged wall hole ( $q = 1.0 \text{ kg/m}$ ) is 0.5m, has been added to Figure 5. In this case, the corresponding PPV over-break limit would be about 1650

mm/sec. The new design curves would suggest that if the charge concentration would be reduced to about 0.65 kg/m, no over-break should occur. There still will be "damage" to the wall rock. This will be discussed later in the paper.

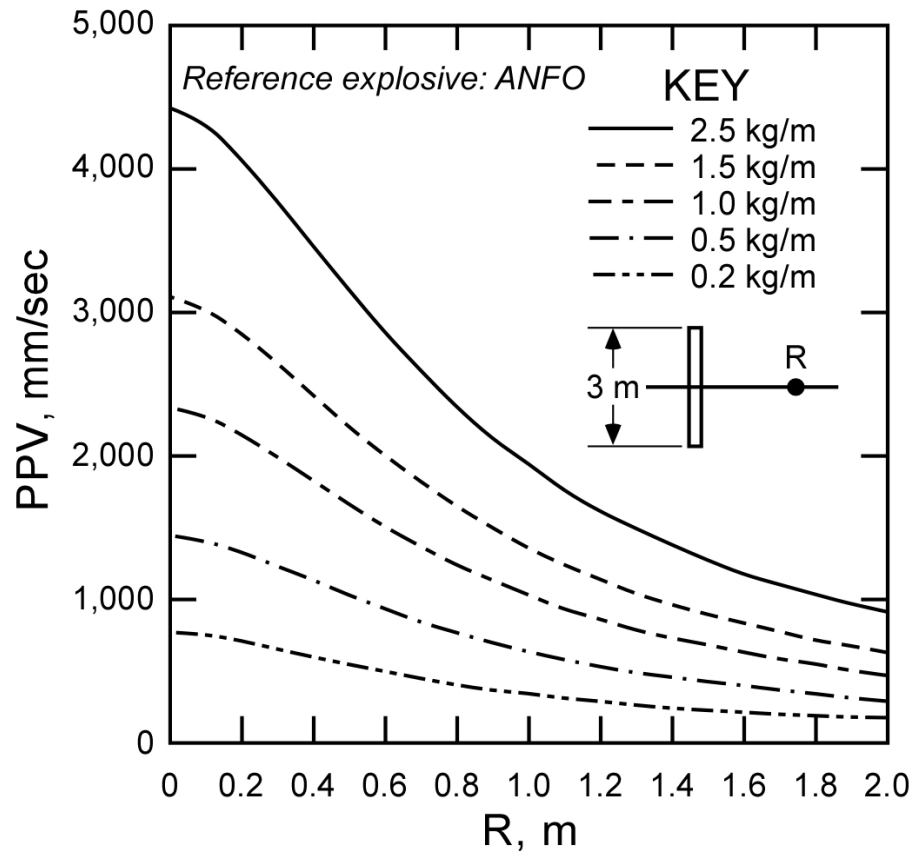


Figure 4. The NIOSH-modified Holmberg-Persson curves for the same conditions as in Figures 2 and 3.

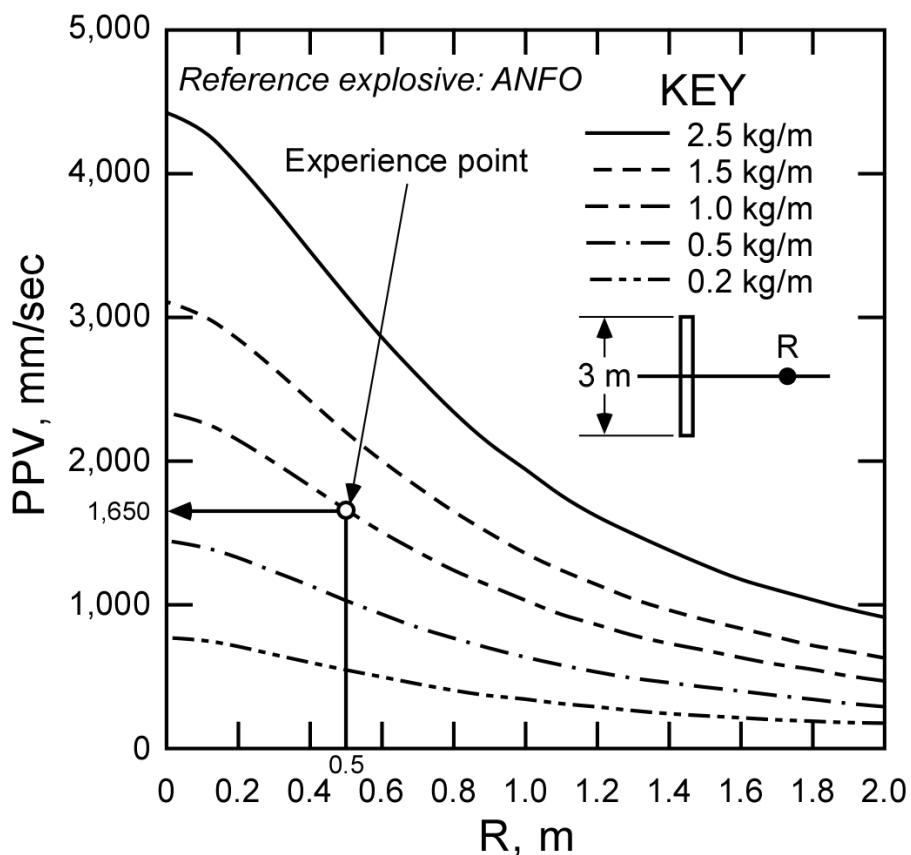


Figure 5. Addition of the experience point to the peak particle velocity versus distance curves of Figure 4.

The conclusion is that although the design curves are somewhat different, the NIOSH modification to the basic Holmberg-Persson approach appears promising. The mathematical problems with the original approach are eliminated with a relatively simple fix.

In practice, one develops the curves for the explosive concentrations of interest and the site constants. One measures the over-break/rock damage. Using this value and the curves, one can determine the limiting PPV. One now has a practical design tool for the site. This procedure will be demonstrated in the following sections.

### 3. Field Data Collection Program

#### 3.1 Introduction

A program of field data collection was conducted at the Stillwater mine, Nye, Montana during July 2006 in conjunction with the blasting of three drift development rounds in the 44W development drift (see Figure 6). The program involved:

- Documenting the drilling and blasting patterns used
- Monitoring the blast vibrations
- Surveying the placement of the blastholes and the final drift contours using a laser-based instrument
- Documenting the rock mass quality

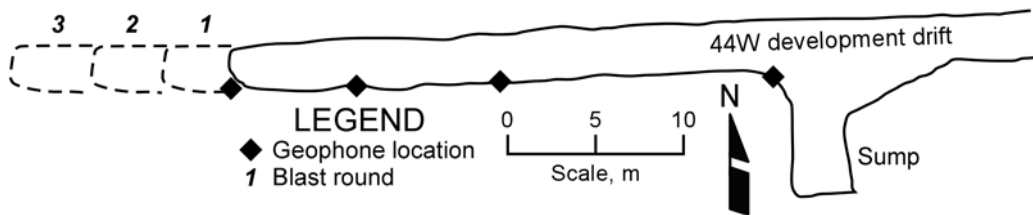


Figure 6. Plan view of the development heading on level 44W in the Stillwater mine showing the locations of the geophones for the three monitored blast rounds. The sump area location is also shown.

The purpose of the field program was to collect the information required for use in the development and application of the NIOSH improved perimeter blast design approach. The rock mass is norite with the following average properties (Johnson et al, 2003):

- Unconfined compressive strength = 103 MPa (15,000 psi)
- Young's modulus = 97 GPa ( $14 \times 10^6$  psi)
- Poisson's ratio = 0.30
- Density = 2.8 g/cm<sup>3</sup>

Over-break measurements from the 4400 and 4700 levels will also be presented.

### 3.2 Drift Round Design

The typical development round blast pattern and delay sequence used at the mine is shown in Figure 7. The nominal drift dimensions are 3.35 m wide by 3.7 m high (crown). The nominal diameter of the blastholes is 48 mm (1-7/8 in. bit) with the uncharged relief holes reamed to 76 mm (3 in.). All holes are drilled to a depth of 4.3m and charged to a length of 3.7 m. The collar is left unstemmed. There are 42 to 43 blast holes and 4 to 6 relief holes in a round depending on the miners' preference for spacing along the back and burn cut pattern. ANFO is used for the burn holes, the production holes and the rib perimeter holes. Dyno AP is used for the lifters and a combination of Dynosplit D and Dyno AP was used in the roof holes.

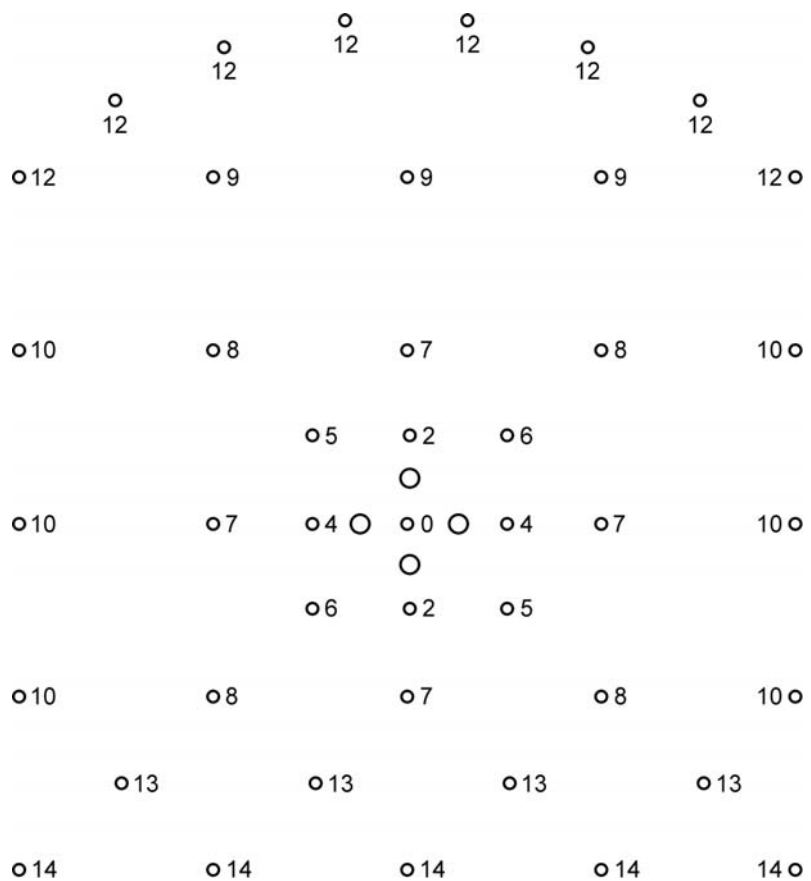


Figure 7. Typical blast pattern for the development heading showing the delay sequence and the relief holes.

Table 1 lists the charge types, weights, number of sticks, relative weight strength based on ANFO, loaded length, and equivalent charge weights per meter of hole. Of the three explosives used, ANFO was the only one that was bulk loaded. There is some uncertainty regarding the charged density, the actual hole diameter, and the charge length. According to the mine, the average amount of ANFO used per hole is 1.9 kg/m (Stillwater Mining Company, 2004). During the mine visit, it was observed that nearly 9 - 22.7 kg bags of ANFO were used to load 30 ANFO holes, or 1.8 kg/m for the second blast round. Other blast rounds monitored by NIOSH personnel during the visit indicated that only 6.0 kg were used per hole or 1.62 kg/m. These latter values will be assumed in the analysis.

Table 1. Calculated charge weights used in the three blast rounds at the Stillwater mine, July 2006.

Explosive charge	Weight per stick, kg	Number of sticks	Total weight, kg	Relative strength compared to ANFO	Explosive charge length, m	Equivalent weight per m, kg/m
<b>Production:</b>						
ANFO <sup>1</sup>	NA	NA	6	1	3.7	1.62
<b>Lifter:</b>						
DynoAP <sup>2</sup>	0.485	11	5.34	0.88	3.7	1.27
<b>Trim:</b>						
DynoAP	0.485	3	1.46	0.88	1.0	1.27
Dynosplit D <sup>3</sup>	0.342	3	1.03	1.13	1.8	0.64
DynoAP	0.485	3	1.46	0.88	1.0	1.27

<sup>1</sup> ANFO – the as-charged specific gravity was 0.84 to 0.89 based on mine report.

<sup>2</sup> Dyno AP - relative weight strength is 0.88. Each 400 mm length by 32 mm diameter stick weighs 0.37 kg

<sup>3</sup> Dynosplit D -- relative weight strength is 1.13. Each 600 mm length by 22 mm diameter stick weighs 0.34 kg (uncoupled charge)

NA - not applicable

A Trojan Stinger primer was placed at the bottom of each ANFO hole. Since the Dyno AP is cap sensitive, no primer was needed in the holes charged with this product. The nominal times associated with the Nonel LP delay detonators used in the design shown in Figure 7 are given in Table 2.

Table 2. Nominal Detonator Delay Times (Dyno Nobel, 2007).

Delay Number	Nominal Delay Time (ms)
0	0
2	800
4	1400
5	1700
6	2000
7	2300
8	2700
9	3100
10	3500
12	4400
13	4900
14	5400

Even though a number of different holes are shot on the same delay, the actual initiation times will generally be different due to cap scatter.

### 3.3 Vibration Measurements

Peak particle velocity (PPV) data were collected from the three sequential blast rounds using an array of triaxial geophones (Instantel™ part number 714A9101). The geophones were surface-mounted along the left rib by drilling a short hole into the rock, installing an anchor bolt, and then attaching the geophone onto the anchor bolt using a washer and nut. Using this attachment method, the geophones were coupled directly to the rock surface in a side-mounted orientation. Figure 8 shows one of the triaxial geophones mounted to the left rib of the development drift. Care was taken to protect the geophone cables from fly rock from the blast rounds and impacts from mobile equipment.

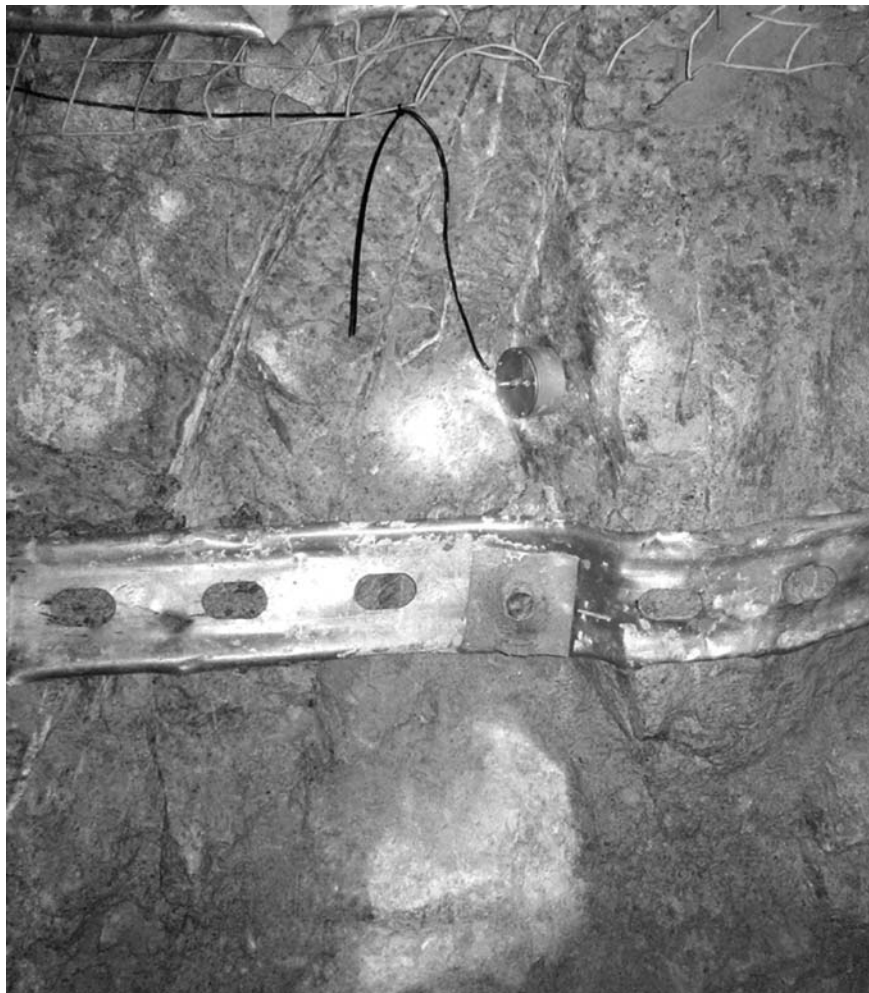


Figure 8. Triaxial geophone mounted to the rock surface using anchor bolt.

Three Instantel Minimate Plus™ data loggers were used to collect particle velocity data. Two triaxial geophones were typically attached to each data logger. Particle velocity data were collected continuously, triggered by the first delay and continuing a full three seconds after the last delay.

For the first round, two geophone locations were used. For round two the number of locations was increased to four. The number of geophone locations in round three was three.

Blastware™ software was used to calculate vector sums of the transverse, vertical, and longitudinal wave forms. PPV was picked from the vector sum data for each arrival in each delay. This was possible because of the scatter effect that occurred from the non-electric delays. PPV data were input into a spreadsheet and identified by arrival time, delay, explosive type, and weight of charge. Except for delay 0 it was not possible to attach a particular arrival time to a particular hole. For each geophone location, the travel distance is assumed equal to the distance from the geophone to the face of the blast plus the distance from the hole collar to the center of the charge as measured along the left rib.

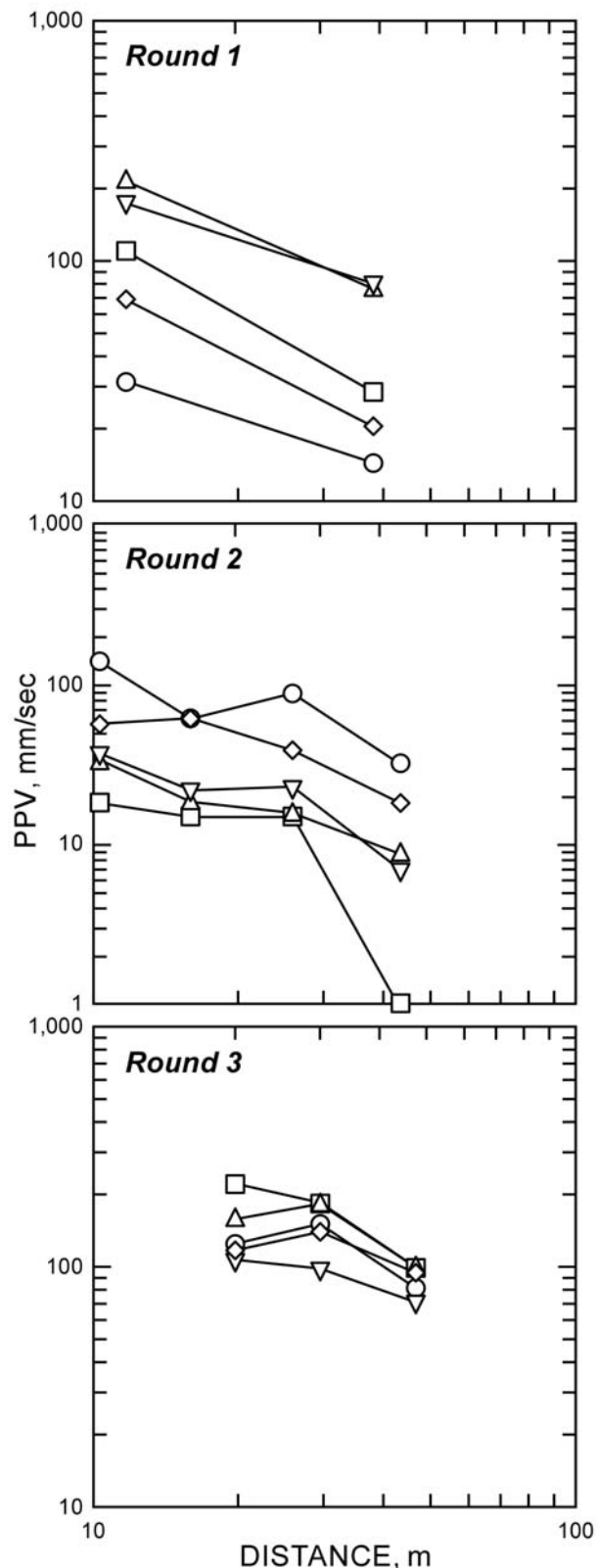


Figure 9. PPV versus distance curves for the lifters by round. The explosive is Dyno AP.

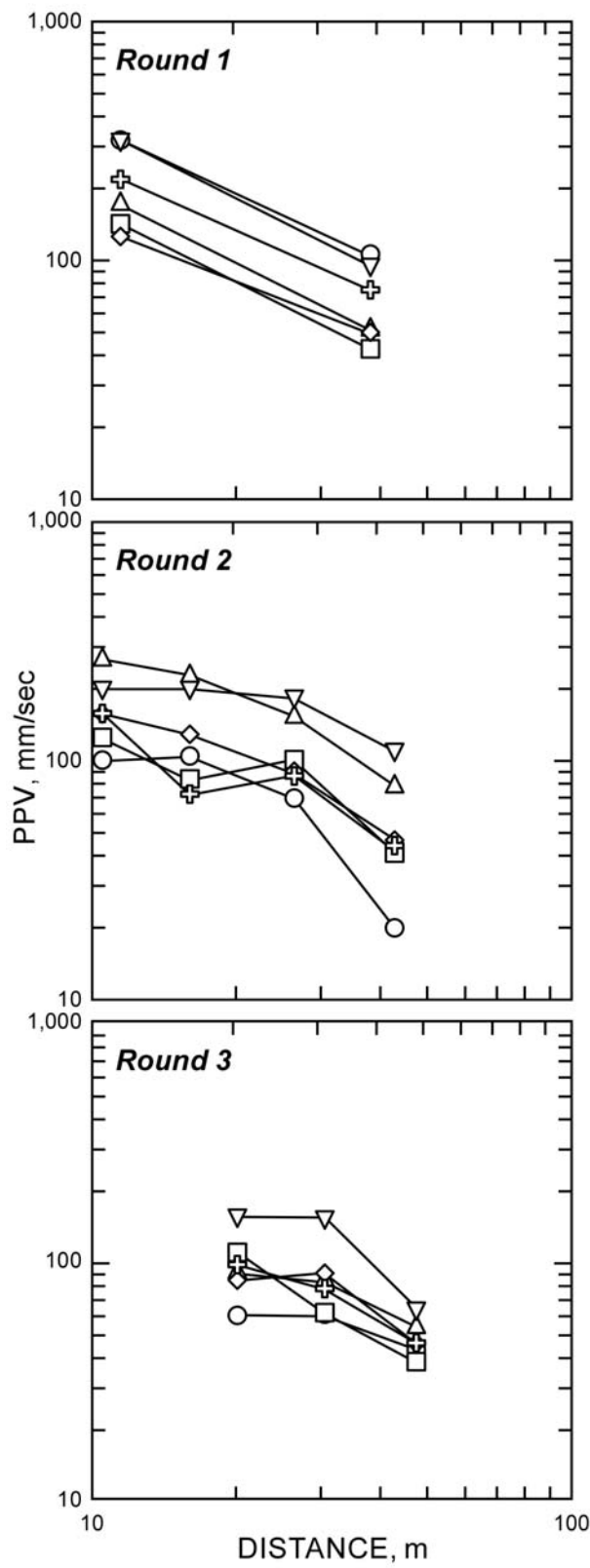


Figure 10. PPV versus distance curves for the rib holes by round. The explosive is ANFO.

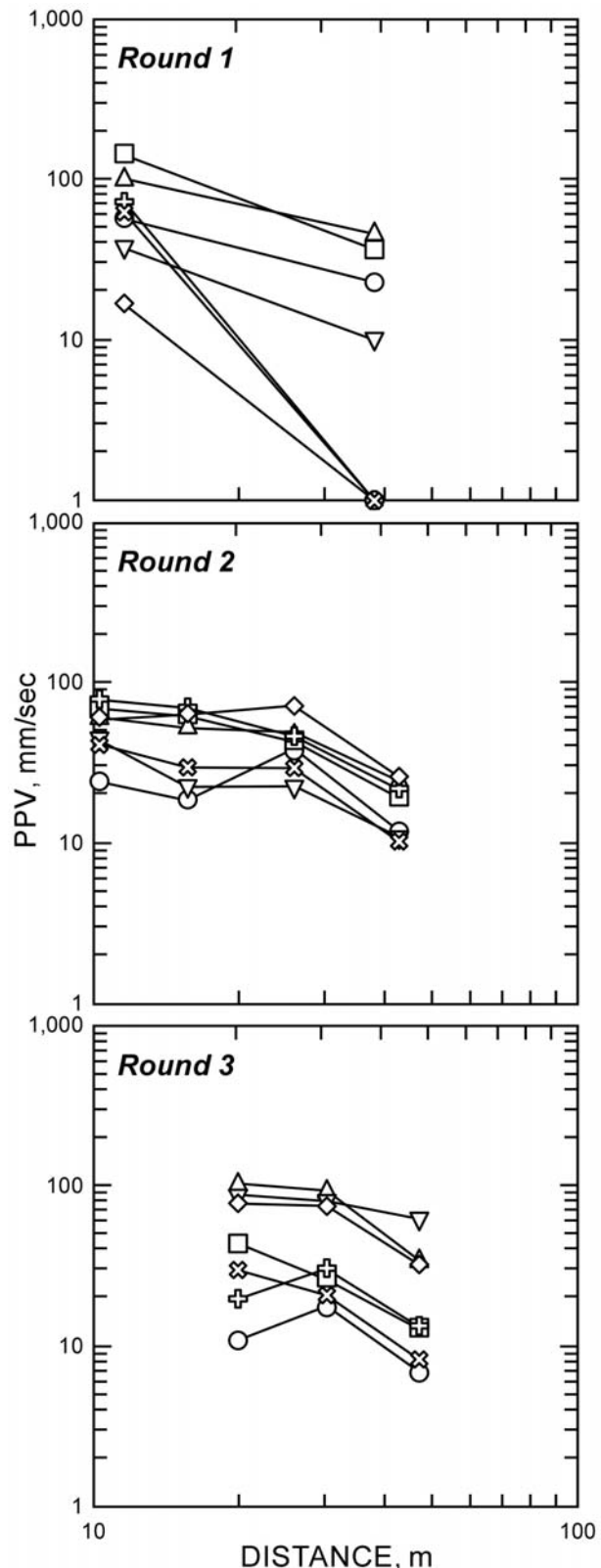


Figure 11. PPV versus distance curves for the roof holes by round. The explosive is a combination of Dynosplit D and Dyno AP.

Figures 9 – 11 show the PPV versus distance results obtained from the lifters, rib and back holes for the three rounds. The analysis of these data will be discussed in the following section.

### 3.4 Over-break measurements

Over-break measurements were based on making a three-dimensional laser scan of the excavation after the blast. Work is progressing on developing a method to obtain the locations of the drill holes in space based upon laser-scanning the blast round face. This method requires scanning the drilled face with tubes/pipes inserted into the holes. The tube orientations obtained from the scans together with the known hole lengths are then used to develop a three-dimensional picture of the actual drill pattern. This pattern is then compared to the post blast scan excavation limit. This method takes time and can interfere with production schedules. Fortunately, one drilled-face scan was made demonstrating this method. A cross-section showing the excavated limit and over-break measurements for an earlier blast round of the sump area is shown in Figure 12. This sump area is also identified in Figure 6. The drill holes were projected into the section and compared with the excavated limit. Over-break due to the ANFO-charged rib holes at this section ranged from 0.39 m to 0.54 m and averaged 0.46 m. Over-break along the back of that blast round was nominal with some half-casts visible.

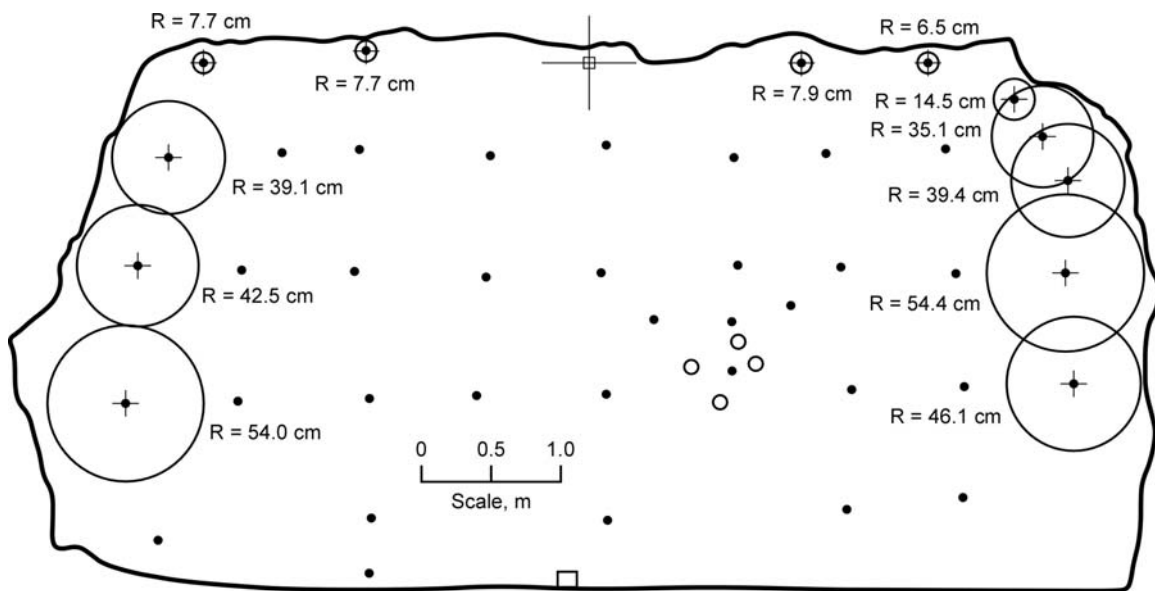


Figure 12. Cross-section through a room at the Stillwater mine showing the hole locations and the final profile as determined using the scanning laser. Level 4400, July 2006.

Several post-blast laser scans were acquired between the sump area and the three blast rounds for which the PPV measurements are reported in this paper. Production schedules and access only during the daytime shifts prevented the use of the laser scanner for drilled-face scans. During the later period, the last two days, no scans were taken. Based on the scans taken, the average rib over-break was determined to be 0.18 m. The theoretical drift width of 3.25 m was subtracted from the average waist-high level scanner measurements. One half of this difference is defined as the representative rib over-break. Blasthole angles were assumed normal to the face and the lookout angle was not considered.

Figures 13 and 14 are additional examples of using the drill hole projections. Figure 13 shows the case when Dynosplit D was used in the left wall and in the roof holes. The right wall was charged with ANFO. In Figure 14, the left wall was charged with ANFO and the right wall and roof holes were charged with Dynosplit D. Although these blast rounds are from a different level in the mine than that on which the PPV measurements were made, the rock type is the same. The average over-break from the ANFO-charged rib holes in these blast round sections was 0.20 m.

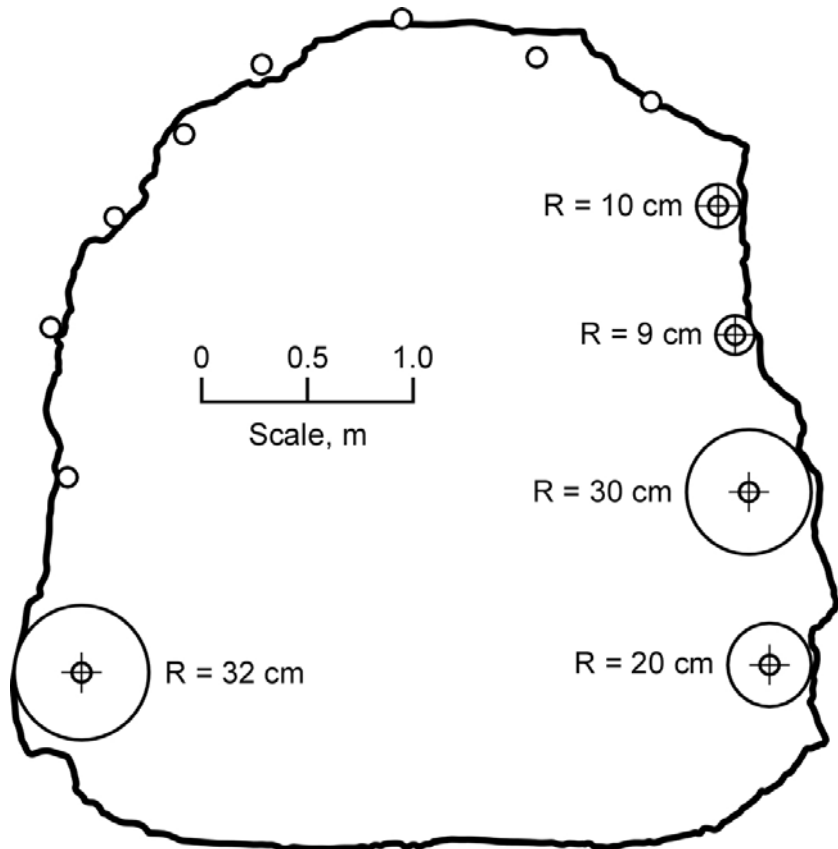


Figure 13. Cross-section through a development round (September 2006). The left rib and the roof holes were charged with DynoSplit D and the right rib with ANFO.

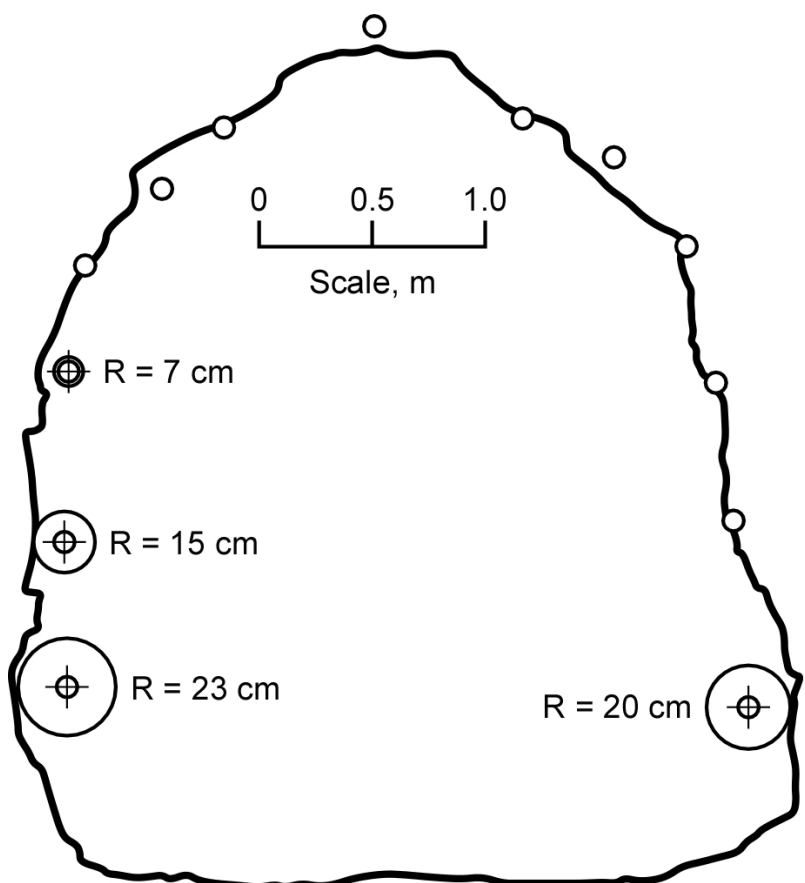


Figure 14. Cross-section through a development round (September 2006). The right rib and roof holes were charged with DynoSplit D and the left rib with ANFO.

The amount of over-break from the ANFO-charged perimeter holes varied depending on location and method of determination. In the sump area, the over-break was quite significant at 0.46 m. For the development headings, the over-break was 0.18 m and 0.20 m at the two locations examined.

#### **4. Analysis of the Vibration Data**

##### **4.1 Introduction**

A new theoretical approach for perimeter blast design based on using  $\bar{R}$  has been presented. The basic equation is

$$PPV = K Q^\alpha / \bar{R}^\beta \quad (11)$$

To apply the approach for drift design at a particular drifting site, values for K,  $\alpha$ , and  $\beta$  are required. The steps for determining these constants using the data from Round 2 will be described in this section together with the application of the technique to the data collected at the Stillwater mine.

##### **4.2 Steps in the Process**

One can write equation (11) as

$$\log_{10} PPV = \log_{10} K + \alpha \log_{10} Q - \beta \log_{10} \bar{R} \quad (12)$$

The first step is to plot  $\log PPV$  versus  $\log \bar{R}$  in  $\log_{10} - \log_{10}$  format for constant Q. In practice, one makes such plots for each of the different explosive charges involved. Figures 9 – 11 shows the curves for the lifter holes, the rib (wall) holes and the roof (back), respectively. In this particular case:

$$Q = 4.69 \text{ kg (lifters)} - \text{Dyno AP}$$

$$Q = 6 \text{ kg (rib holes)} - \text{ANFO}$$

$$Q = 3.72 \text{ kg (roof) holes} - \text{Combination of Dyno AP and Dynosplit D}$$

The explosives differ in energy content per unit weight and thus a normalization with respect to ANFO is performed. This reference explosive should be clearly indicated in the upper corner of the resulting design curves.

As indicated earlier, the problem which immediately arises is the selection of the distance to be chosen. From the simple plan view of the roof holes shown in Figure 15, it is clear that the waves from the different holes must travel different distances to arrive at the monitoring points. Although some assumptions might be made in that regard, it will be assumed that all are placed at the center of charge for the hole closest to the wall. One might think that the pulse from the hole at the wall would be the first arrival because it has the shortest distance to travel. This however is not necessarily the case because the lack of precision of non-electric delays results in a distribution of actual detonation times. The nearest detonation could be the last to arrive. The solution is, for a given charge, the highest amplitude should be associated with the closest holes. Those further away would have lower amplitudes. This is considered to be the most important reason for the apparent “spread” in amplitudes. Taking an “average” value to represent the holes is not considered correct. Rather, the most regular curve of highest amplitude was chosen to represent each charge group.

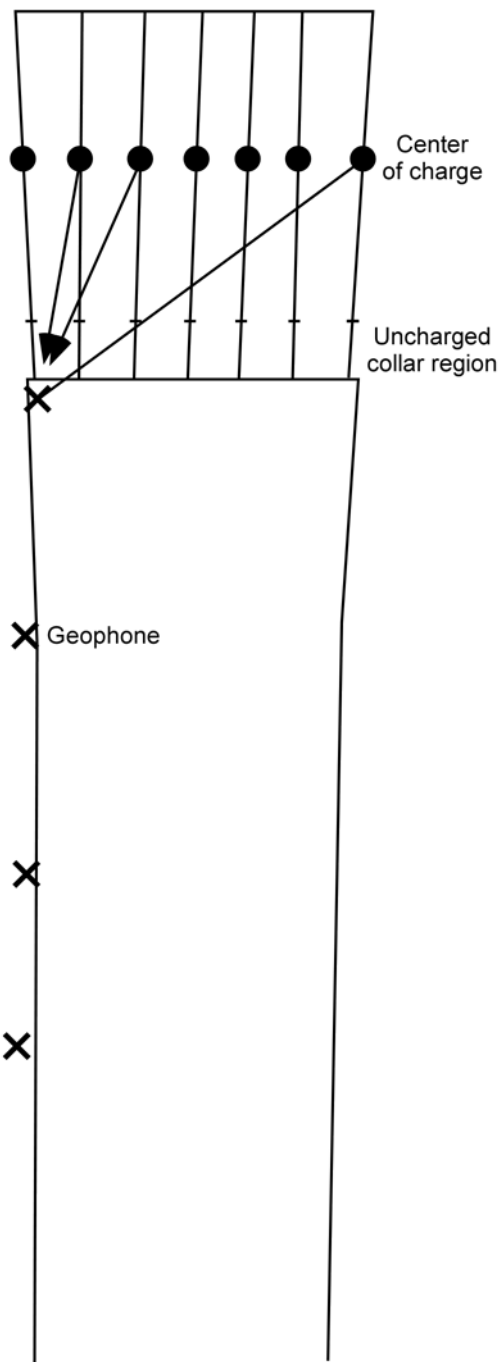


Figure 15. Diagrammatic representation of one set of possible paths for the seismic waves traveling from the roof holes to the rib-mounted geophones.

From viewing the log PPV versus log distance plots (including those for the production holes (not shown)), it was found that a slope of -1 could describe the data very well. The slope is represented by the constant

$$\beta = 1$$

shown in equation (11). This suggests that in the medium to far field (where the measurements are being made), the charge in each hole can be represented by an equivalent sphere. As a result, a best fit straight line curve of slope -1 was placed through each of the selected curves as shown in Figure 16.

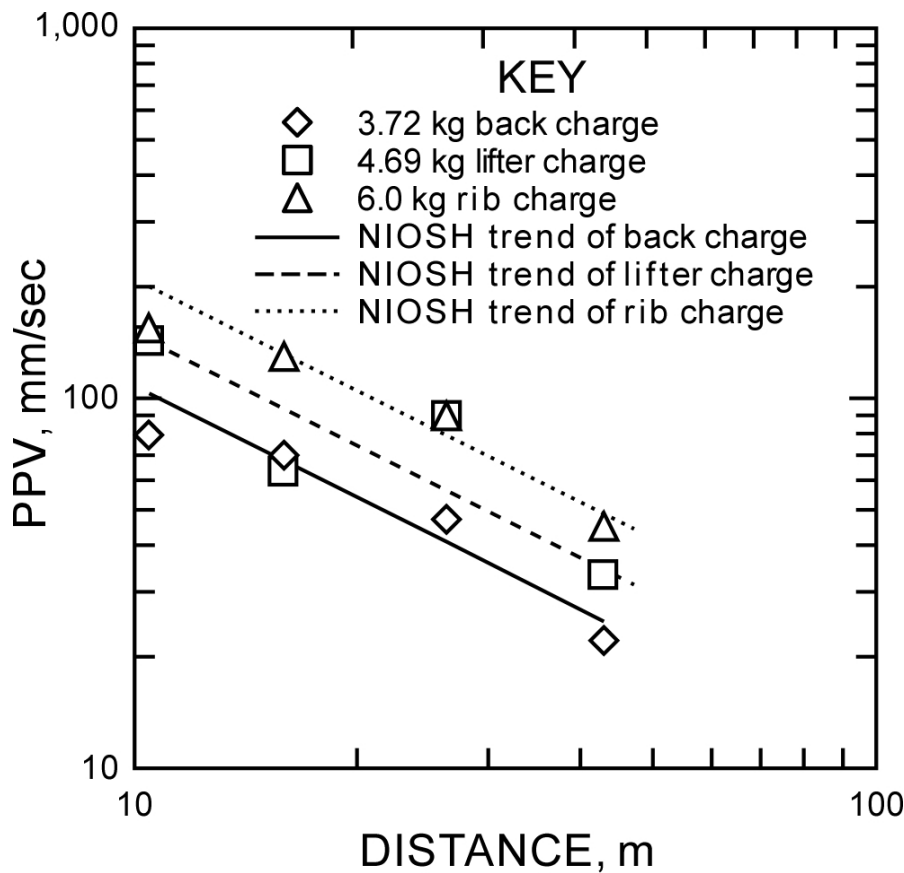


Figure 16. PPV versus distance for the rib, lifter and roof holes. The maximum amplitude curve has been selected.

For these charge lengths and distances,  $R \approx \bar{R}$ . For a given value of  $R$ , the values of PPV for the different  $Q$  values are read from the curves. In this case,

$$R = 15 \text{ m}$$

was chosen. The values are

$Q$ (kg)	PPV (mm/s)
3.72	50
4.69	75
6.00	96

In returning to the basic equation

$$\log_{10} \text{PPV} = \log_{10} K + \alpha \log_{10} Q - \beta \log_{10} \bar{R} \quad (12)$$

it can be seen that with  $K$  constant and  $\bar{R}$  constant, the  $\log_{10}\text{PPV}$  versus  $\log_{10}Q$  should plot as a straight line with slope  $\alpha$ . This plot is shown in Figure 17.

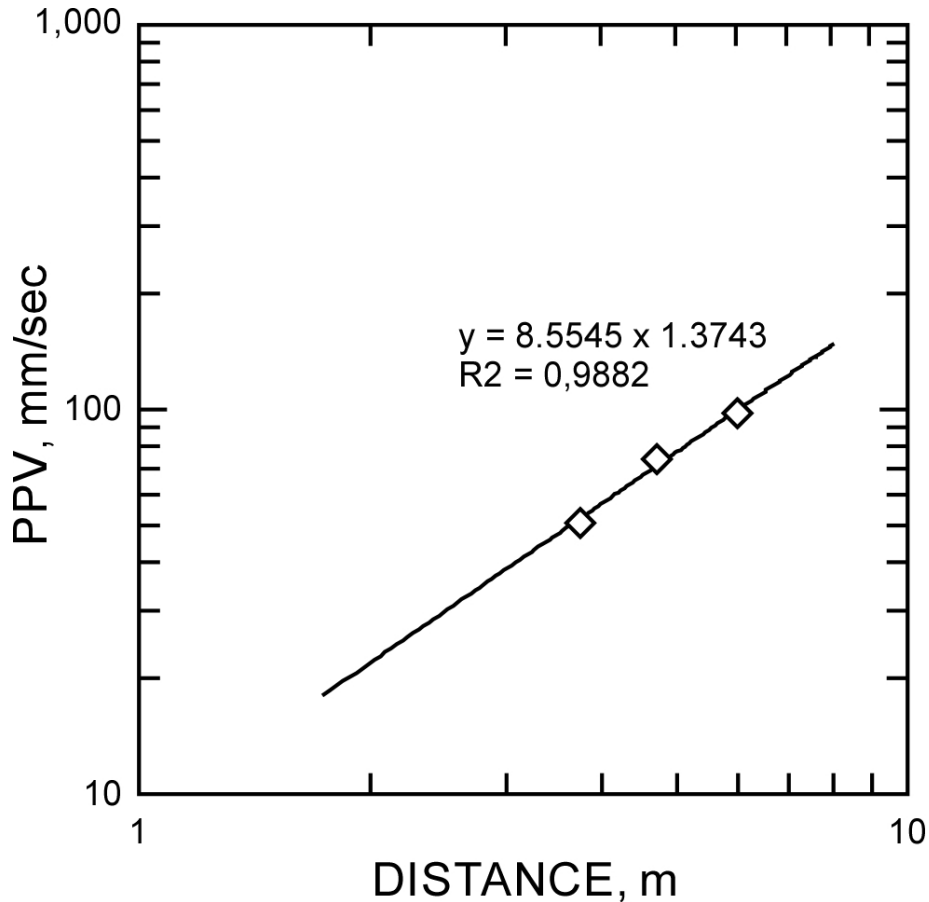


Figure 17. PPV versus Q for  $R = 15$  m. Round 2.

The slope is determined to be

$$\alpha = 1.4$$

knowing

$$\alpha = 1.4$$

and

$$\beta = 1$$

one can solve for K. In this particular case it is

$$K = 171$$

The final design equation becomes

$$PPV = 171 (qL)^{1.4} / \bar{R}$$

Since the charge length is

$$L = 3.7 \text{ m}$$

the charge concentrations for the different charge groups become

Charge Group	$q (\text{kg/m})$
Rib holes	1.62
Lifters	1.27
Back holes	1.00

The design curves for each of these charge concentrations are shown in Figure 18.

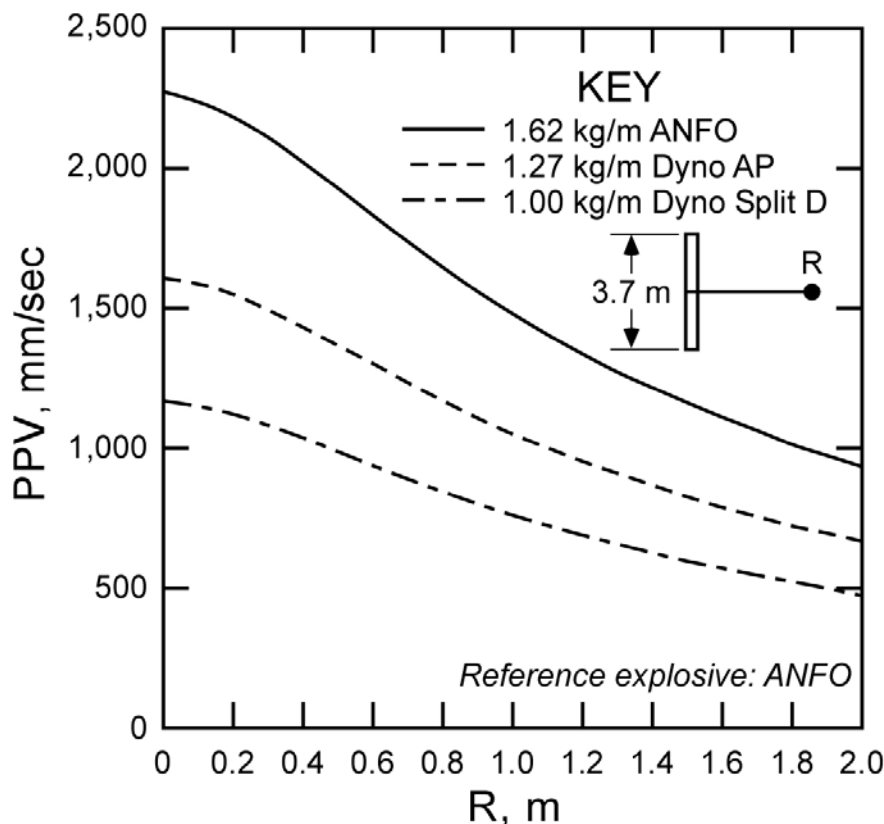


Figure 18. The NIOSH-modified Holmberg-Persson curves using the site constants determined for the Stillwater mine.  $L = 3.7$  m.

#### 4.3 Limiting PPV Values

For the ANFO loaded wall holes in Figure 12, the amount of over-break is of the order of

$$OB = 0.5 \text{ m}$$

where OB is the over-break.

For the Dyno AP/Dynosplit D loaded roof holes the over-break was minimal. Applying this information to the design chart shown in Figure 19, it is seen that the

$$\text{PPV limit} = 1850 \text{ mm/s}$$

Since the maximum calculated PPV for the roof holes is only 1170mm/s, no over-break was expected and such was the case.

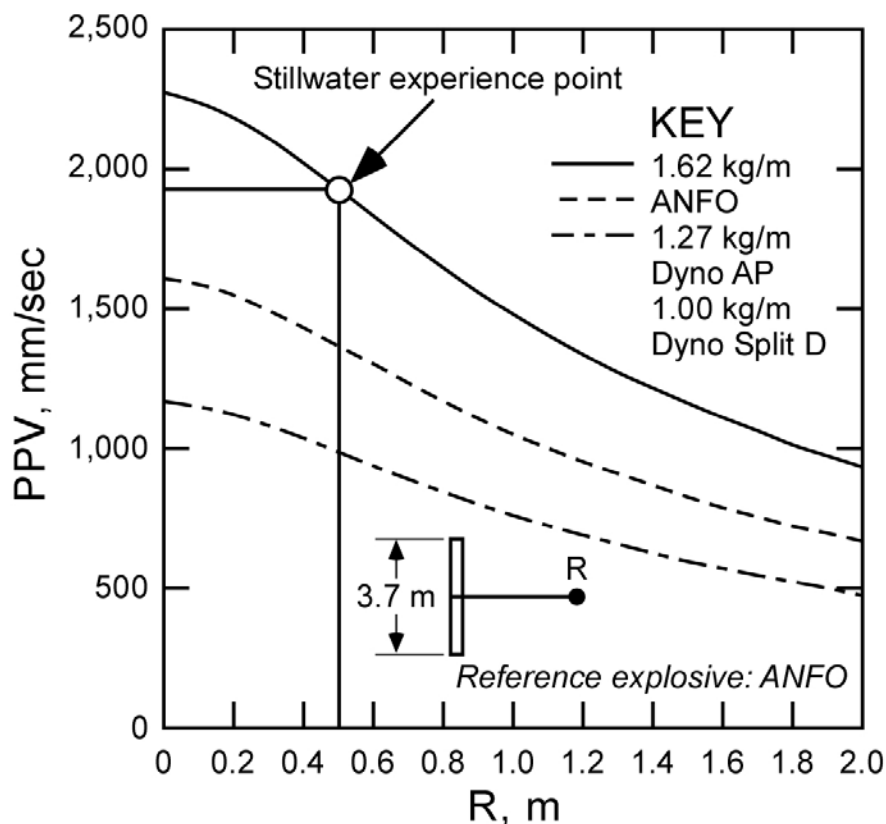


Figure 19. Addition of the experience point to the peak particle velocity versus distance curves of Figure 18.

#### 4.4 Definition of Undesired Blast Damage

In this paper, the amount of over-break (excavation outside of the line of perimeter holes) has been selected as the measure of undesired blast damage since it could be easily quantified using the laser scanner. This is the simplest measure and the one easiest for miners to understand since it can be directly translated into economic terms due to (1) the additional scaling time required, (2) the extra muck to be moved, and (3) the need for extra reinforcement due to wider spans and higher walls. For civil engineers, it may translate into the need to replace the removed rock with concrete. Over-break can be easily quantified using normal surveying techniques. The PPV limits assigned on this basis using the NIOSH-modified Holmberg-Persson design curves apply to over-break and hence one should use the notation  $PPV_{lim}$  (over-break). From the Stillwater mine results, this limit appears to be

$$PPV_{lim} \text{ (over-break)} = 1850 \text{ mm/s}$$

Holmberg and Persson have designated the limiting PPV based on new crack formation in the surrounding rock mass. Using their design curves they found that

$$PPV_{lim} \text{ (new crack formation)} = 700 - 1000 \text{ mm/s}$$

for Swedish igneous rocks. By simply applying the 1000 mm/s limit to the design curves developed for the Stillwater mine based on the current work (see Figure 20), one would predict the following cracking limits:

Holes	Explosive	Extent of Cracking (m)
Rib	ANFO	1.8
Lifters	Dyno AP	1.1
Roof	Dynosplit D/ Dyno AP	0.5

These seem quite high and future NIOSH field work will incorporate techniques to try and quantify the cracking limit as well as the over-break limit. At this point in time, primary reliance will be based on application of the Micro-Velocity Probe. The results will be the subject of a future paper.

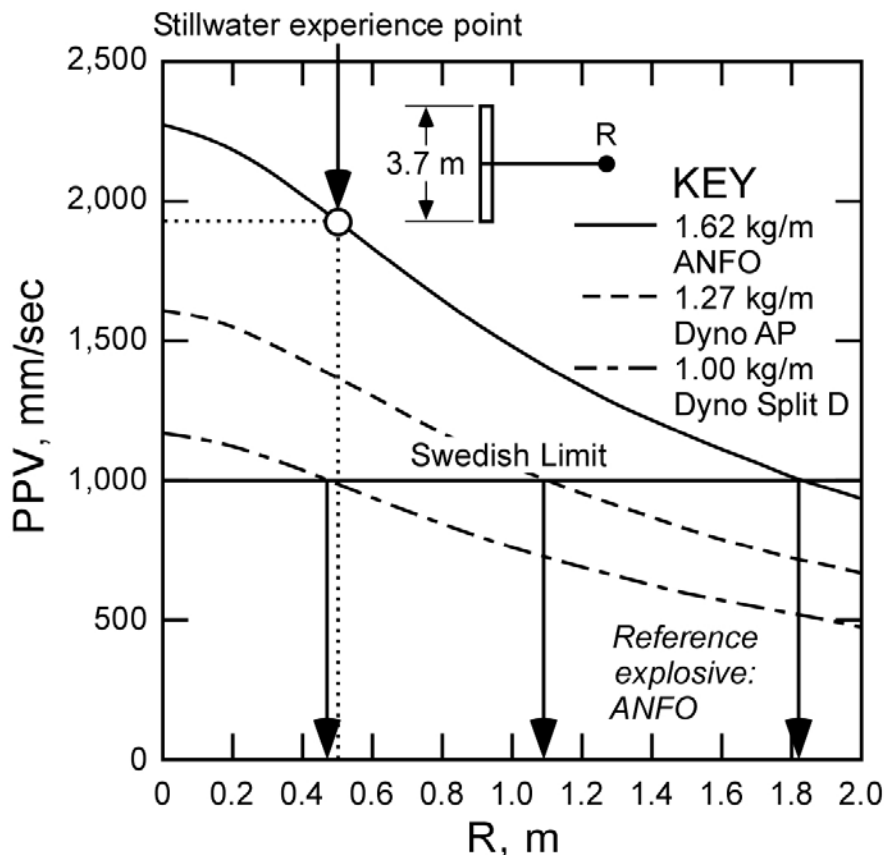


Figure 20. Addition of the Swedish granite fracture damage limit to the peak particle velocity versus distance curves of Figure 18.

## 5. Summary and Conclusions

The Holmberg-Persson perimeter blast design approach has found widespread use since its introduction in 1978. It is logical and easy to apply. Unfortunately, a recently discovered mistake in their equation development has raised questions regarding the whole procedure. As part of a comprehensive perimeter blast design research and development program, NIOSH has reviewed the basics of the Holmberg-Persson design approach and has introduced the modification described in this paper which retains the simplicity of the procedure while correcting the mathematical problems. The NIOSH-modified Holmberg-Persson design curves, although slightly different in appearance from those originally presented by Holmberg-Persson, are easy to develop and use.

The basis for the design approach is the peak particle velocity expressed as

$$PPV = KQ^\alpha / R^\beta$$

where

PPV = peak particle velocity

Q = charge weight

R = distance

$\alpha, \beta$  = constants

To be able to use the design approach, one must select values for the constants. One way has simply been to assume the values suggested by Holmberg-Persson:

PPV = peak particle velocity (mm/s)

Q = charge weight (kg)

R = distance (m)

K = 700

$\alpha$  = 0.7

$\beta$  = 1.5

Another way is to make site measurements of PPV recorded at different distances from a drift blast round. From the captured signals, the PPV values corresponding to the different explosive charge weights are identified. NIOSH has used this latter procedure at the Stillwater mine. The details of the approach needed to extract the constants have been provided. One of the interesting findings is that  $\beta$ , the power of the distance, can be well represented by

$$\beta = 1$$

This is quite logical since for the far field measurements ( $R \gg$  charge length) typically made in the mine environment, the charge may be represented by a sphere. The task then becomes one of finding K and  $\alpha$ . The practical steps needed to accomplish this are provided in the paper. The PPV versus distance design curves with the linear charge concentration, q, as a parameter based upon the Stillwater site constants have been included.

The final step in the process is the determination of the limiting PPV values. A scanning laser has been used to survey the blast rounds prior to firing to locate the blast holes in space and again after firing to determine the final contour. From these scans, the amount of over-break can be determined. In one test, the average over-break for the ANFO-charged wall holes was about 0.5m. Using the design curves one finds that

$$PPV_{lim} (\text{over-break}) = 1850 \text{ mm/s}$$

Applying this limit to the roof holes charged with a combination of Dynosplit D and Dyno AP, one would not expect any over-break. The measured over-break was of the order of 0.1m which could have been due to the ANFO-charged buffer row.

Identification of the new fracture formation limit and the calculation of

$$PPV_{lim} (\text{new crack formation})$$

is part of the continuing NIOSH research and development program. The new perimeter blast design procedures described in this paper are being incorporated in a special drift blast design software package.

NIOSH is currently expanding the study by making measurements at a number of other mines.

## **6. Acknowledgements**

The authors acknowledge the Stillwater Mining Company and specifically the help of Radford Langston and John Marjerison for providing two active development drifts to facilitate research in monitoring the blast vibrations and measuring over-break. NIOSH personnel and contractors involved in the research and data collection included Edward McHugh, Tom Brady, Rimas Pakalnis, Timothy Orr, Cristian Caceras, Jami Dwyer, Phillip Joggerst, and Joel Warneke.

## **7. References**

Dyno Nobel. 2007. [www.dynonobel.com](http://www.dynonobel.com).

Weast, R. C. (editor-in-chief), 1983, Handbook of Chemistry and Physics, 64<sup>th</sup> edition, 1983-1984, CRC Press, Inc.

Holmberg, R., and P-A. Persson. 1978. The Swedish approach to contour blasting. Proceedings of the 4<sup>th</sup> Conference on Explosives and Blasting Technique. SEE. Pp 113-127.

Holmberg, R., and P-A. Persson. 1979. Design of tunnel perimeter blasthole patterns to prevent rock damage. Proceedings, Tunneling '79. Editor, M J. Jones. Institution of Mining and Metallurgy, London, UK.

Holmberg, R., and W. Hustrulid. 1981. Swedish cautious blast excavation at the CSM/ONWI test site in Colorado. Pp 232-252. Proceedings, 7<sup>th</sup> Conference on Explosives and Blasting Technique. SEE.

Holmberg, R. 1982. Charge calculations for tunneling. Section 7.5: Blasting, Chapter 1. Underground Mining Methods Handbook (W.A. Hustrulid, editor). SME. 1982. pp 1580-1589.

Hustrulid, W., and R. Holmberg. 1991. Drilling and Blasting. Chapter 5 in Underground Structures – Design and Construction (R.S. Sinha, editor). Elsevier. Pp 141-223.

Hustrulid, W., and W. Lu. 2002. Some General Design Concepts Regarding the Control of Blast-Induced Damage During Rock Slope Excavation. Proceedings, FragBlast7. Beijing, China.

Hustrulid, W, 2004, “Evaluate the Effects of Blasthole Loading Accuracy and Over-break in Various Geologic Environments”, Final Report – NIOSH Contract S0265130, October 31.

Johnson, J., T. Brady, M. MacLaughlin, R. Langston, and H. Kirsten, 2003, “In Situ Stress Measurements at the Stillwater Mine, Nye, Montana”, in Soil and Rock America 2003, 12th Pan-American Conference on Soil Mechanics and Geotechnical Engineering and the 39th U.S. Rock Mechanics Symposium, Volume 1, Cambridge, MA, Massachusetts Institute of Technology, 2003, pp. 337-344.

Knutti, T. 2007. Personal communication. Dyno Nobel. August.

Lundborg, N., Holmberg, R., and P-A. Persson. 1978. The dependence of ground vibrations on distance and charge size. Report R11:78. Byggforskning. In Swedish.

Martin, P.A. 2007. Personal communication. Department of Mathematical and Computer Sciences. Colorado School of Mines. August.

Persson, P.A., R. Holmberg and J. Lee, 1994, "Rock Blasting and Explosives Engineering", CRC Press, 540 pp.

Stillwater Mining Company, 2004, "Report on Drill and Blast Audit at the Stillwater Mining Company, Nye Mine", Confidential report, 22 pp.